© 2017 IJSRST | Volume 3 | Issue 7 | Print ISSN: 2395-6011 | Online ISSN: 2395-602X
Themed Section: Science and Technology

Predictive Direct Angle Control of Induction Motor Fed from Five level Diode Clamped Multilevel Inverter

Dubba Sree Lakshmi, B. Thejasvi
Department of Electrical and Electronics Engineering, Jawaharlal Nehru Technological University, Anantapur, Anantapur, Andhra Pradesh, India

ABSTRACT

This paper represents a Finite control set model predictive control (FCS-MPC) has been recognized as a capable and reasonable procedure in factor speed drive applications. Considering the discrete should of the converters and using a cost work for state assurance diminishes the computational weight not withstanding having a correct control. In this paper FCS-MPC has been used to develop a novel technique for induction motor control. Conflictingly to customary direct torque and transition control, in the proposed methodology the torque and the point between stator current and rotor movement are controlled. The movements are not simply controlled. A five-level Diode clamped multilevel inverters topology is applied on induction motor control known as direct angle control strategy. More inverter states can be generated by a five-level inverter which improves voltage selection capability. This paper also introduces two different control methods to select the appropriate output voltage vector for reducing the torque and flux error to zero. This technique manufactures the efficiency of the motor in light loads without using on the web perfect flux estimation. The angle control has being achievable by using FCS-MPC without constraining time consuming calculations. Closed loop desire show is used to construct the precision of the prediction angle. A novel and simple gain calculation is in like manner proposed. The proposed procedure has been evaluated by the two simulation and experiments.

Keywords : Finite Control Set Model Predictive Control, FOC, GPC, MPC, DTC, FCMI, CHMI, NPC

I. INTRODUCTION

Demonstrate predictive direct torque control has been examined as an option for regular motor control strategies, and field oriented control (FOC). Predictive control may come about into quicker unique reaction and exact constant state reaction too. Distinctive sort of predictive control strategies have been examined to date. Two primary gatherings of predictive control that has been connected in drive applications are miscreant control and model predictive control (MPC). Deadbeat control depends on voltage computation with the point of correct reference following [1] and [2]. This technique is not strong against parameter variety on the grounds that the discrete idea of the inverter is not considered in the calculations. MPC depends on a cost work which comprises of criteria for references following. The cost capacity should to be limited for voltage computation.

The minimization procedure can be performed by methods for two strategies, i.e., generalized up predictive control (GPC) and Finite control set model predictive control (FCS-MPC). In GPC technique [3] and [4], the minimization depends on exchange work based controlled auto regressive integrated moving average (CARIMA) show. This technique incorporates overwhelming calculations and is not predominantly utilized as a part of drive applications. In FCS-MPC technique [5]-[9], the discrete idea of inverter is considered and minimization is best on picking the best feasible alternative. This strategy is anything but difficult to execute and the outcomes are persuading. In this way, FCS-MPC can understand the trademark downsides of DTC, for example, high torque swells with protecting the advantages of DTC. In any case, one disadvantage of DTC can't be unraveled by utilizing predictive DTC. This disadvantage blocks the ideal and decoupled control and causes bring down proficiency for predictive DTC contrasted with FOC.

The strategy in [11] repays the parameter variety of the machine. An online iterative calculation should to be executed for this technique. Besides, singular look into tables should to be accomplished for each machine. The technique proposed in [13] depends on signal injection of pulsating current space vector superimposed. Demonstrate predictive control has been used for current minimization in [14]-[16]. Be that as it may, since FCS-MPC rearranges the cost work minimization, other criteria could be added to the cost work. In [14] and [15], the criteria of MTPA and current confinement are added to the cost work.

The first invention in multilevel converters was the so-called neutral point clamped inverter. It was initially proposed as a three level inverter. It has been shown that the principle of diode clamping can extended to any level. The main advantages and disadvantages of this topology are: Advantages: High efficiency for the fundamental switching frequency. The capacitors can be pre-charged together at the desired voltage level. The capacitance requirement of the inverter is minimized due to all phases sharing a common DC link. Keeping in mind the end goal to restrain the voltage in rapid operations, voltage minimization paradigm is included [16]. In these strategies, the criteria of MPTA are in field oriented casing. At that point, outline transmission is required and mistake of casing introduction will diminish the exactness. Then again no less than three criteria are added to the cost work. In this manner, the calculations are expanded and the affectability and many-sided quality of the control strategy is like FOC technique. The ideal operation is added to the cost work with just a novel point control paradigm. No immediate flux control is performed in this technique. Along these lines, there will be just two criteria in the cost work like ordinary MPC. The strategy is produced for enlistment motor control.

In order to reach to a precise control for developing angle control, closed loop prediction model is used. The proposed method is described in section II. The closed loop prediction model is presented in section III and the results are presented in section IV.

II. PREDICTIVE DIRECT ANGLE CONTROL

A. Concept

Ordinary limited control set model depends on cost work minimization. The cost work comprises of torque and flux blunder those should to be limited. The greater parts of the feasible states are tried in the cost capacity and best choice is connected. In all immediate torque control techniques, the torque control couldn't be performed without flux control. The accompanying condition demonstrates the ward of the torque to the flux.

$$T = \frac{3}{2} p \left|\overrightarrow{\lambda s}\right| \left|\vec{I}s\right| \sin\alpha_s \quad (1)$$

where T is the electromagnetic torque, $\overrightarrow{\lambda s}$ is the stator flux, $\vec{I}s$ is the stator current, α_s is the phase angle difference between stator flux and current, and p is the number of pair poles.

In customary strategy the stator flux is controlled to be nominal value. In this way, the augmentation of $\left|\vec{I}s\right|$ and $\sin\alpha_s$ should to be controlled for torque control. The ideal flux calculation in predictive control has been explored in [17]. Likewise in this technique the flux is controlled on the figured value. At that point, the free factors for ideal control are the current and its stage prediction. Considering this flexibility, it would be conceivable that the transition value is the ideal value yet the present extent is not on account of its duplication by $\sin\alpha_s$ is being controlled. Then again, ideal transition estimation is a complicated procedure.

In this paper a novel control plot is proposed. On the off chance that the stage prediction of the current is controlled to limit the current, the torque control will naturally optimize the flux.

In order to calculate the desired phase angle of the stator current the torque condition is acquired as a component of rotor flux and the stator current.

$$T = \frac{3}{2} p \frac{Lm}{Lr} \left|\overrightarrow{\lambda r}\right| \left|\vec{I}s\right| \sin\alpha_r \quad (2)$$

Where λ_r is rotor flux, L_r and L_m are the rotor and mutual inductances, respectively, and α_r is the phase angle difference between rotor flux and stator current. Equation (2) can be written in rotor flux oriented frame as

$$T = \frac{3}{2} p \frac{Lm}{Lr} \lambda r \, Isq' \quad (3)$$

Where $\lambda r = \lambda rd'$ and the quadratic component of rotor flux is zero.

On the other hand, the rotor's difference equation on the direct axis of the rotor flux oriented frame is

$$R_r I_{rd'} + \frac{d}{dt}\boldsymbol{\lambda}_{rd'} = (\omega_s - \omega_r)\boldsymbol{\lambda}_{rq'} \quad (4)$$

Where R_r is the rotor resistance, ω_s and ω_r are the synchronous and rotor rakish frequencies, separately. In this condition, the correct side term is zero in view of the introduction of the prediction. The subordinate of rotor flux could be accepted zero in constant state condition. Therefore,

$$I_{rd'} = 0 \qquad (5)$$

Therefore, the rotor flux can be calculated as

$$\lambda_r = L_m I_{sd'} \qquad (6)$$

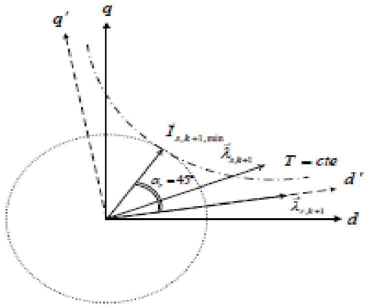

Figure 1. Optimal operation of induction motor

Considering (3) and (6), the torque will be proportional to the multiplication of the stator current components.

$$T = \frac{3}{2} p \frac{Lm^2}{Lr} \, Isd' \, Isq' \ (7)$$

It can be deduced from (7) that the locus of the stator current is a hyperbolic for a constant torque. Then again, the locus is a circle for a constant current size. Along these lines, the base current will happen when the stage point between the stator current and rotor flux is 45º. Fig. 1 demonstrates the vector outline of the fluxes and the current for an induction motor.

B. Control Method

FCS-MPC depends on cost work minimization. This is performed by means of looking at practical states and picking the best applies. The accompanying condition demonstrates the proposed novel cost works which guarantee the torque control and the present minimization.

$$C_j = \left|T^* - \hat{T}_{j,k+1}\right| + Q\left|\hat{\alpha}_{r\,j,k+1} - \pi/4\right|$$

$$\hat{\alpha}_{r\,j,\,k+1} = \angle\overleftarrow{\hat{I}}_{sj,k+1} - \angle\overleftarrow{\hat{\lambda}}_{sj,k+1} \quad j=1,2,\ldots 7 \qquad (8)$$

where, $\widehat{Tj}_{k+1}$ is the predicted torque. $\angle\vec{\hat{I}}_{sj,k+1}$ and $\angle\vec{\hat{\lambda}}_{rj,k+1}$ are the predicted phase angles for the stator current and rotor flux, respectively. Superscript "^" is used for calculated variables. The variables without that are the measured variables. Q is the weighting factor that determines the importance of angle control compared to torque control. The predictions should be performed for 7 feasible voltage vectors (VVs) of a two-level voltage source inverter. j shows the number of the predicting state for j^{th} VV. The voltage vector that limits the cost capacity will be the best apply. This strategy is known as limited control set MPC.

The second term of the proposed cost work decides the bearing of the stator current and the principal term decides the greatness of it. Indeed, the proposed cost work implements the stator current parts to take after their ideal values.. Thus, this cost function automatically includes $\left|\lambda_{sopt}{}^{*} - \left|\vec{\hat{\lambda}}rj,k+1\right|\right|$ and there is no need for direct flux control. The predictions are performed in stationary frame. This will improve the robustness and decrease the calculations.

III. CLOSED LOOP PREDICTION MODEL

With a specific end goal to look at attainable VVs in the proposed cost work (8), the following stage torque and points should to be anticipated. This is performed by considering the specific VV as the contribution of the machine demonstrate. This model should to have the capacity to anticipate the required factors in the subsequent stage. The accuracy of the expectation demonstrate enhances the advancement procedure and prompts better decisions.

The discrete model of induction motor is acquired from the persistent one [18].

$$\frac{\partial}{\partial t}\hat{\lambda}_s = \vec{v}_s - R_s\vec{I}_s \qquad (9\text{-a})$$

$$\frac{\partial}{\partial t}\hat{\lambda}_r = -R_r\vec{I}_r + j\omega_r\overleftarrow{\lambda}_r \quad (9\text{-b})$$

$$\overleftarrow{\lambda}_r = L_r I_r + L_m I_s \qquad (9\text{-c})$$

$$\vec{I}_r = \frac{1}{Lm}(\overleftarrow{\lambda}_s - L_s\vec{I}_s) \quad (9\text{-d})$$

The discretized form of (9) is developed by using Euler method and substituting (9-c) in (9-b).

$$\overleftarrow{\hat{\lambda}}_{sj,k+1} = \overleftarrow{\hat{\lambda}}_{s,k} + t_s(\vec{V}_{s,k} - Rs\vec{I}_{s,k}) \qquad (10\text{-a})$$

$$\vec{I}_{r,k+1} = \left(1 - \frac{t_s}{\tau_r} + j\omega_r t_s\right)\overleftarrow{I}_{r,k} - \frac{Lm}{Lr}\overleftarrow{\hat{I}}_{s,k+1} + \left(\frac{Lm}{Lr}(1 + j\omega_r t_s)\right)\vec{I}_{s,k} \qquad (10\text{-b})$$

The rotor current can be eliminated in (10-b) by substituting (9-d) in it.

$$\vec{I}_{s,k+1} = \frac{1}{\sigma L_s}\hat{\overleftarrow{\lambda}}_{s,k+1} - \frac{1}{\sigma L_s}(1-\frac{t_s}{\tau_r}+j\omega_r t_s)\hat{\overleftarrow{\lambda}}_{s,k} \quad (11)$$

Where $\sigma = 1 - L_m^2/L_s L_r$.

The discrete time model of the induction motor will be utilized as a part of the forecast display. In the event that both of the distinction conditions of the motor are utilized, the model is known as full request display. On the off chance that one the specified conditions is utilized and alternate parameters are computed by mathematical conditions the model is known as decreased request demonstrate. In this classification, if the model that comprises of the stator voltage is utilized, it is known as stator model or voltage show. On the off chance that the second condition that does not comprise of the stator voltage is utilized, it is known as rotor model or current model. Both the full request show and the diminished request demonstrate are broadly being examined for onlooker applications in which the coveted factors are evaluated at the present time. These models can likewise be utilized for state forecast applications too. Between the lessened request models, the voltage show is more common due to less many-sided quality.

The voltage display has the accompanying downsides contrasted with full request demonstrate: 1) immersion issue as a result of info dc counterbalance; 2) yield dc balance on account of starting blunder; and 3) affectability to the stator-resistance, particularly at low speeds [19]. Then again, the yield would be more exact and robust in the full request demonstrate since both of the distinction conditions of the machine are considered [7]. On the off chance that the blunder of estimation is engaged with the model, the eyewitness will be known as "closed loop onlooker [18]. Discrete types of closed spectator has been researched to date. In [20], a Kalman channel based closed loop spectator is utilized.

In this paper the closed loop full request demonstrate is utilized to predict the

$$\hat{\overleftarrow{\lambda}}_{sj,k+1} = \hat{\overleftarrow{\lambda}}_{s,k} + t_s(\vec{V}_{s,k} - Rs\vec{I}_{s,k}) + K_{p1}\, t_s(\vec{I}_s - \hat{\overleftarrow{I}}_{sp}) \quad (12\text{-a})$$

$$\vec{I}_{s,k+1} = \frac{1}{\sigma L_s}\hat{\overleftarrow{\lambda}}_{s,k+1} - \frac{1}{\sigma L_s}(1-\frac{t_s}{\tau_r}+j\omega_r t_s)\hat{\overleftarrow{\lambda}}_{s,k} + (1-\frac{t_s}{\sigma\tau_r}+j\omega_r t_s)\vec{I}_s + K_{p2}\, t_s(\vec{I}_s - \hat{\overleftarrow{I}}_{sp}) \quad (12\text{-b})$$

Where τ_r is rotor time constant, $\overrightarrow{I_s}$ and $\hat{\vec{I}}_{sp}$ are the measured and the last predicted current, respectively. Kp1 and Kp2 are the coefficients of the feedback.

For the next step rotor flux prediction the second difference equation of the motor is used.

$$\vec{I}_{r,k+1} = (1-\frac{t_s}{\tau_r}+j\omega_r t_s)\vec{I}_{r,k} + \frac{Lm}{Lr}(1+j\omega_r t_s)\vec{I}_s - \frac{Lm}{Lr}\hat{\overleftarrow{I}}_{s,k+1} \quad (13)$$

On the other hand relationship among flux and currents is

$$\hat{\overleftarrow{\lambda}}_{rj,k+1} = L_r\hat{\overleftarrow{I}}_{r,k+1} + L_m\hat{\overleftarrow{I}}_{s,k+1} \quad (14)$$

Equations (13) and (14) leads to the rotor flux prediction equation.

$$\hat{\overleftarrow{\lambda}}_{rj,k+1} = \frac{Lr}{Lm}(1-\frac{t_s}{\tau_r}+j\omega_r t_s)\hat{\overleftarrow{\lambda}}_{s,k}) + \left\{\sigma L_m(1+j\omega_r t_s) - \frac{LsLr}{Lm}\frac{t_s}{\tau_r}\right\}\vec{I}_s \quad (15)$$

Equation (15) shows that the subsequent stage rotor flux is not identified with the VV that will be picked. Consequently, just the extent and the stage point of the stator current will be determinative for the VV choice in the cost work. This enhances the techniques robust in light of the fact that the reasonable blunder of the forecast demonstrate influences just the stator current vector. The inspecting VV will likewise influence the anticipated torque by means of the stator current vector as it were.

$$\hat{T}_{k+1} = \frac{3}{2}p\frac{Lm}{Lr}|\overrightarrow{\lambda r}||\vec{I}s|\sin\hat{\alpha}_{r,k+1} \quad (16\text{-a})$$

$$\hat{\alpha}_{rj,k+1} = \angle\hat{\overleftarrow{I}}_{s,k+1} - \angle\hat{\overleftarrow{\lambda}}_{r,k+1} \quad (16\text{-b})$$

Fig.2 shows the block diagram of the proposed method. It is depicted that the present time flux is estimated by the state observer block. The closed loop prediction model is used to predict next step torque and its phase angle difference for seven feasible voltage vectors.

In the writing, three sorts of multilevel inverters have been utilized as a part of DTC with Imposed Switching Frequency methodology; FCMI, CHMI and asymmetry/half breed CHMI. When all is said in done, the exchanging recurrence burden methodology is performed by considering the momentary estimations of torque and transition and their subsidiaries for the determination of space vector. A predictive model is dictated by inferring the evaluated estimations of torque and transition, which are ascertained from the deliberate estimations of IM factors, versus time.

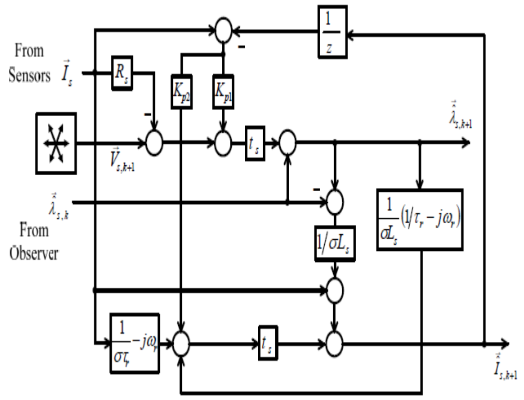

Figure 2. Block diagram of the closed loop prediction model

Multilevel Inverter (MLI)

The quantity of accessible space voltage vectors is expanded by relatively to the voltage levels of the inverter. By utilizing a multilevel inverter in the traditional plan of IM, a more exact control of torque and flux can be accomplished from additional adaptability in choosing the ideal voltage vector. The three-stage multilevel inverter is a mix of three multilevel inverter legs. There are three essential multilevel inverter topologies: Diode-braced multilevel inverter (DCMI) or impartial point cinched (NPC) inverter, Flying Capacitor multilevel inverter (FCMI), and Cascaded H-Bridge multilevel inverter (CHMI).

Note that the block diagram of the state onlooker is like the expectation display outline. In any case, torque and rotor transition estimation is not required in the demonstration. Subsequently, (12) should to be postponed and utilized. With a specific end goal to delineate the procedure of the proposed technique

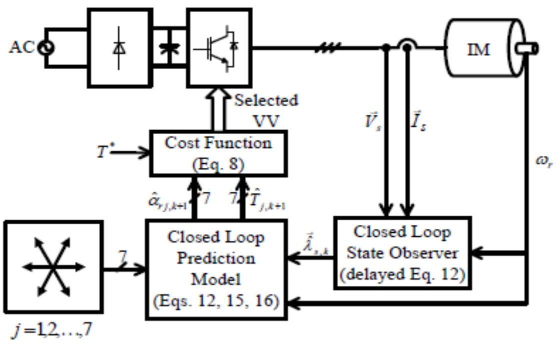

Figure 3. shows the detailed block diagram of the closed loop prediction model.

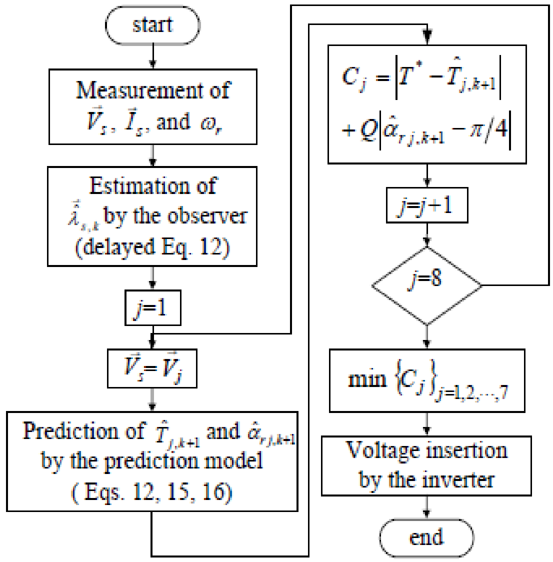

Figure 4. Flow diagram of the predictive direct angle control method

IV. Feedback Gain Calculation

Criticism of the closed loop forecast model may expand the robust of the strategy. Along these lines, no iterative strategies will be expected to compensated the parameter variety in the present minimization strategy. In this paper a novel and straightforward strategy is utilized. The post moving strategy is proposed for sensorless DTC. Thus, no large shift of the poles is needed. Large shift will place the slow poles so far from the quadratic axes which will slow the prediction model.

Note that the speed is measured in the proposed predictive direct prediction control strategy. Accordingly, no huge move of the shafts is required. Extensive move will put the moderate shafts so distant from the quadratic axes which will moderate the forecast demonstrate. For compromising between the quickness and dependability of the forecast show, the shifting value k_{sh}, is determined by H-infinity robustness equation.

The feedback gains in (12) are complex values.

$$K_{p1}=K_{p11}+jK_{p12} \quad K_{p2}=K_{p21}+jK_{p22} \quad (17)$$

The real and imaginary parts of the gains are calculated to shift the poles of the prediction model with respect to poles of

the motor.

$$K_{p11}=\mathrm{Re}\left\{\frac{k_{sh}(k_{sh}-a_2)}{a_1}\right\}$$

$$K_{p12}=\mathrm{Im}\left\{\frac{k_{sh}(k_{sh}-a_2)}{a_1}\right\} \qquad (18\text{-a})$$

$$K_{p21}=2k_{sh}\ ,\ K_{p22}=0 \qquad (18\text{-b})$$

In order to determine ksh , the H-infinity norm of the discrete transfer function of the closed loop model is minimized.

$$\text{Min } k_{sh}\|C(zI-A')^{-1}B\|_{\infty} \quad (19)$$

Where

$$A'=\begin{bmatrix} 1 & -t_s R_s - t_s K_{p1} \\ t_s a_1 & 1 + t_s a_2 - t_s K_{p2} \end{bmatrix} \quad (20\text{-a})$$

$$B=t_s\begin{bmatrix} 1 \\ 1/\sigma L_s \end{bmatrix} \quad (20\text{-b})$$

$$C=[0\ 1] \quad (20\text{-c})$$

A suboptimal solution of (19) attains when the following equation is solved [24].

$$\|C(zI-A')^{-1}B\|_{\infty} \leq \frac{1}{\|\Delta A'\|} \quad (21\text{-a})$$

$$\Delta A' = t_s\begin{bmatrix} 0 & -\Delta R_s \\ \frac{\Delta R_r}{L_r} & -\frac{1}{\sigma}\left(\frac{\Delta R_s}{L_s}+\frac{\Delta R_r}{L_r}\right) \end{bmatrix} \quad (21\text{-b})$$

Considering 100% changes for the stator and the rotor resistances, the right side term of (21-a) will be 0.08447. Since grid A1 is a speed subordinate one, condition (21-an) should to be illuminated in a decided speed. It is appeared in [7] that the most pessimistic scenario of power is in zero speed in onlooker applications. In any case, (21-a) won't have an answer in that speed. By inspecting low speed go, it is found that ω=50 r/min (3% of the nominal synchronous speed) is the base speed that (21-a) has an answer. Fig. 5 demonstrates the variety of the interminability standard of the closed loop exchange work when the move value shifts from 50 to 100. It can be seen that the interminability standard is diminished when the move value is expanded. With a specific end goal to dodge vast move values which will moderate the expectation demonstrate, the condition purpose of (21-an) is considered. In this way, the ideal move value is equivalent to 72. Note that the figured increases should be multiplied by ts =100µsec ts for using in discrete model. The eigen values of the discrete time model with that sample time will be 0.8843 ± j0.0001 and 0.8756 ± j0.0001 which are inside the unit loop. If the sample time is increased the closed loop system will be less accurate. The limit for the sampling time in order to keep the poles inside unit loop is 1.607 msec.

i. Pre-Magnetization In The Start-Up Stage

Since there is no immediate flux control in the proposed strategy, in this way, just in the startup organize, it is unrealistic to keep the torque at zero and increment the transition. This will diminish the dynamic speed of the torque reaction toward the start-up organize. A start-up polarization technique is proposed to beat this issue. In this stage the reference estimation of the stage prediction is set to zero rather than 45 degree. By considering Fig. 1, it can be found that zero stage prediction will build the transition while keeping the torque on the zero value. Keeping in mind the end goal to make the transition expanded, the zero voltage vector is dispensed with from practical voltage vector at this stage.

$$C_j = \left|T^* - \hat{T}_{j,k+1}\right| + Q\left|\hat{\alpha}_{r\,j,k+1} - 0\right|$$

$$\hat{\alpha}_{r\,j,k+1} = \angle\overleftarrow{\hat{I}}_{sj,k+1} - \angle\overleftarrow{\hat{\lambda}}_{sj,k+1} \quad j=1,2,\ldots 6 \quad (22)$$

Additionally, the typical type of the proposed technique should to be applied when the transition achieves its nominal value, with a specific end goal to maintain a strategic distance from immersion. Indeed, the primary chose dynamic voltage vector will be chosen persistently until the point when the transition spans to its nominal value. A while later, the ordinary type of the proposed technique is proceeded. Here, the start-up cost work Is shown.

Diode-clamped multilevel inverter

The diode-clamped inverter provides multiple voltage levels through connection of the phases to a series bank of capacitors. According to the original invention, the concept can be extended to any number of levels by increasing the number of capacitors. Early descriptions of this topology were limited to three-levels where two capacitors are connected across the dc bus resulting in one additional level. The additional level was the neutral point of the dc bus, so the terminology neutral point clamped (NPC) inverter was introduced. However, with an even number of voltage levels, the neutral point is not accessible, and the term multiple point clamped (MPC) is sometimes applied. Due to capacitor voltage balancing issues.

Figure (5). Shows the topology of the five-level diode-clamped inverter. Although the structure is more complicated than the two-level inverter, the operation is straightforward and well known. Labels S_{a1} and S_{a2} are used to identify the transistors as well as the transistor logic (1=on and 0=off). Since the transistors are always switched in pairs, the complement transistors are labeled S_{a1} and S_{a2} accordingly. In a practical implementation, some dead time is inserted between the transistor signals and their complements meaning that both transistors in a complementary pair may be switched off for a small amount of time during a transition. However, for the discussion here in, the dead time will be ignored. From Figure (5), it can be seen that, with this switching state, the a-phase current ias will flow into the junction through diode as D_{a1} if it is negative or out of the junction through diode D_{a2} if the current is are positive. According to this description, the inverter relationships for the presented in Table.1.

Table.1 Five level Inverter Relationships

Voltage V_{a0}	Switch state									
	S_{a5}	S_{a4}	S_{a3}	S_{a2}	S_{a1}	$S_{a'5}$	$S_{a'4}$	$S_{a'3}$	$S_{a'2}$	$S_{a'1}$
$V_5 = 5V_{dc}$	1	1	1	1	1	0	0	0	0	0
$V_4 = 4V_{dc}$	0	1	1	1	1	1	0	0	0	0
$V_3 = 3V_{dc}$	0	0	1	1	1	1	1	0	0	0
$V_2 = 2V_{dc}$	0	0	0	1	1	1	1	1	0	0
$V_1 = 1V_{dc}$	0	0	0	0	1	1	1	1	1	0
$V_0 = 0$	0	0	0	0	0	1	1	1	1	1

If each capacitor is charged to one-half of the dc voltage, then the line-to-ground and voltage can be calculated. The general n-level modulator, described in the next section, determines the switching state for each phase. For practical implementation, the switching state needs to be converted into transistor signals.

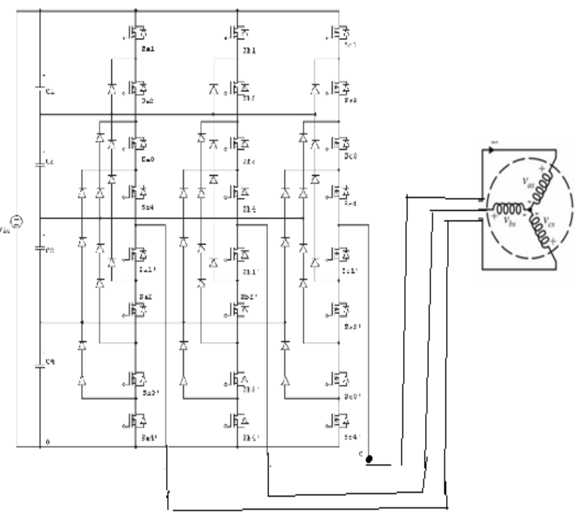

Figure 5. Five-level Diode clamped inverter topology

Considering Table.1, this can be accomplished in general by

$$T_{at} = \begin{cases} 1 & s_a \geq i \\ 0 & elsewhere \end{cases} \qquad (23)$$

An inverse relationship may also be useful and is given by

$$s_a = \sum_{i=1}^{n-1} T_{at} \qquad (24)$$

Once the transistor signals are established, general expressions for the a-phase line to- ground voltage and the a-phase component of the dc currents can be

$$v_{ag} = \sum_{i=1}^{n-1} T_{at} V_{ct} \qquad (25)$$

written as

$$\boldsymbol{i_{adci}} = \left[T_{a(t+1)} - T_{at}\right] i_{at} \qquad \text{for i=1,2,…(n-2)} \quad (26)$$

V. SIMULATION RESULTS

Conventional Results :

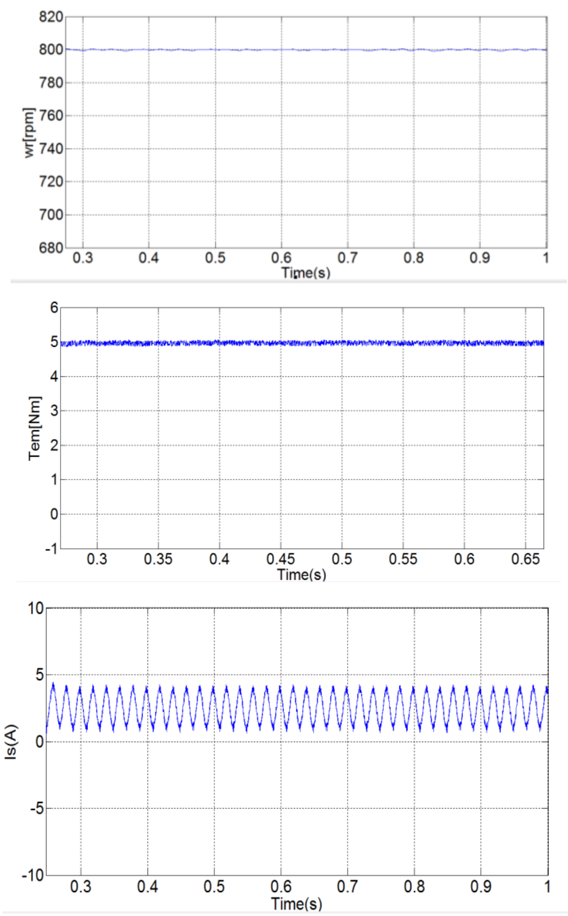

Figure 6. Steady state responses of the conventional predictive direct angle control

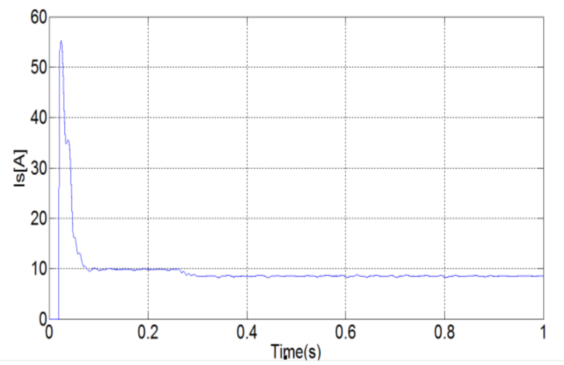

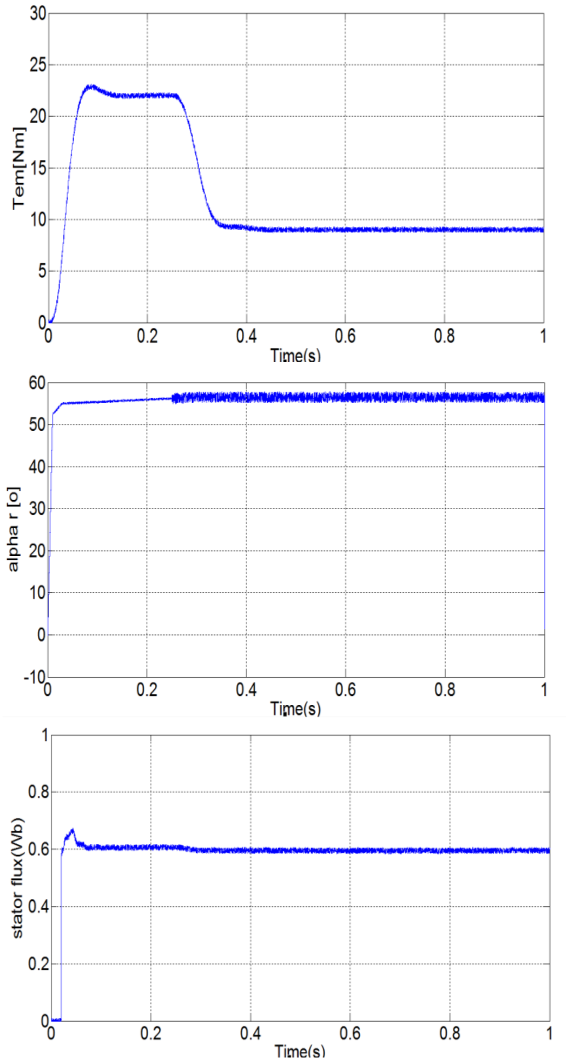

Figure 7. Dynamic state response of the conventional predictive direct angle Control

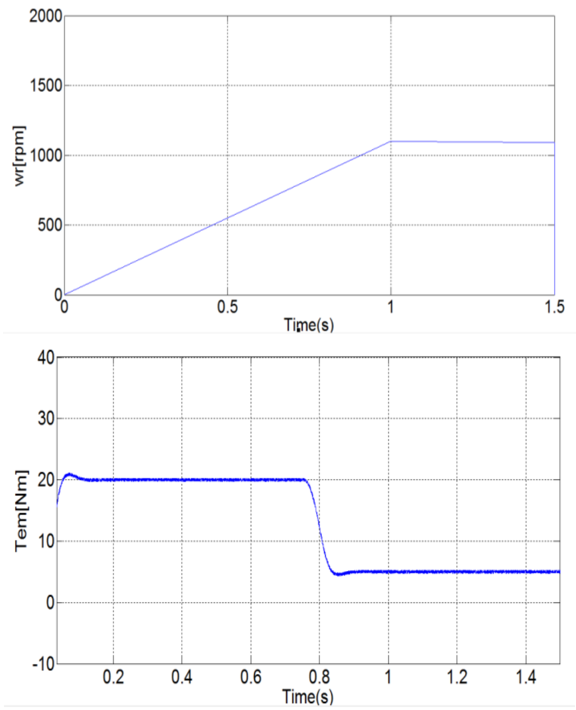

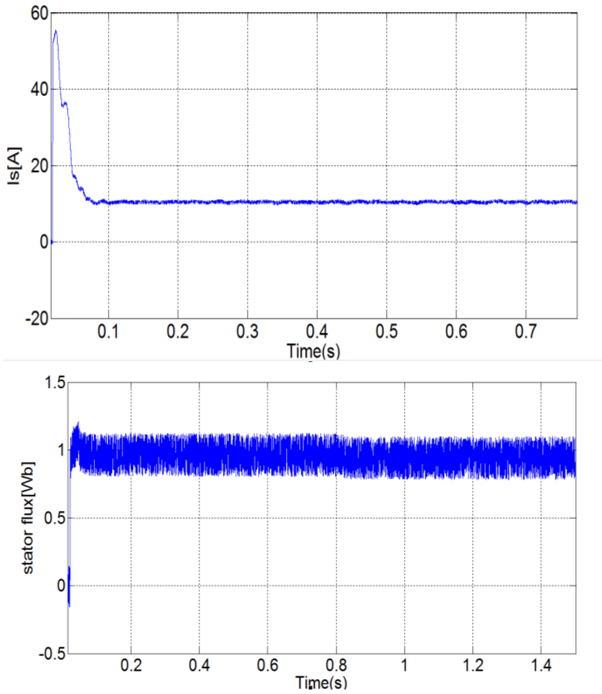

Figure 8. Full load condition responses of the conventional predictive direct angle control

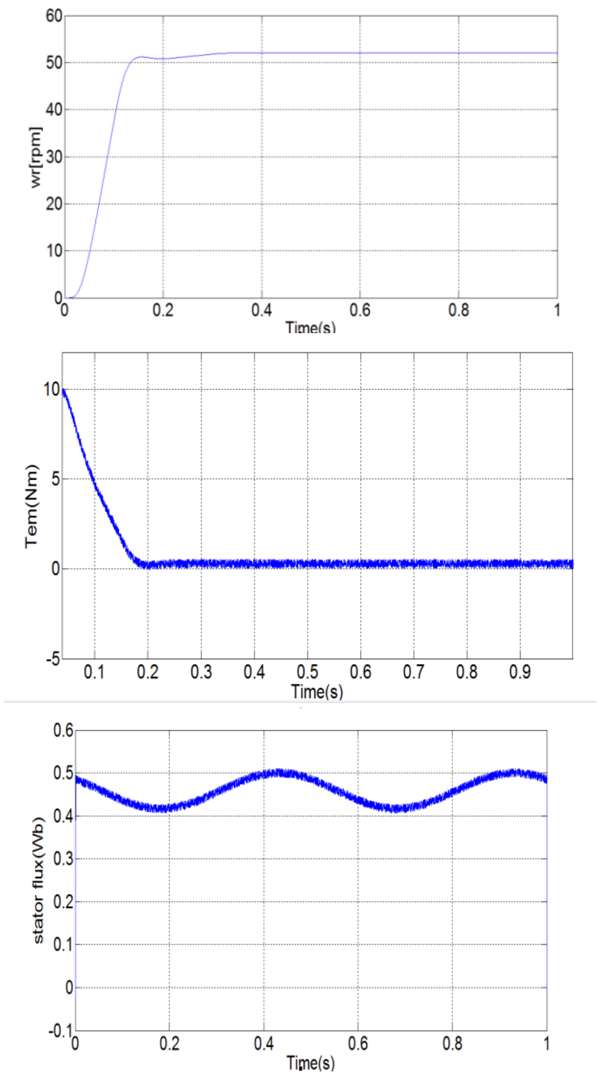

Figure 9. Light load condition responses of the conventional predictive direct angle control

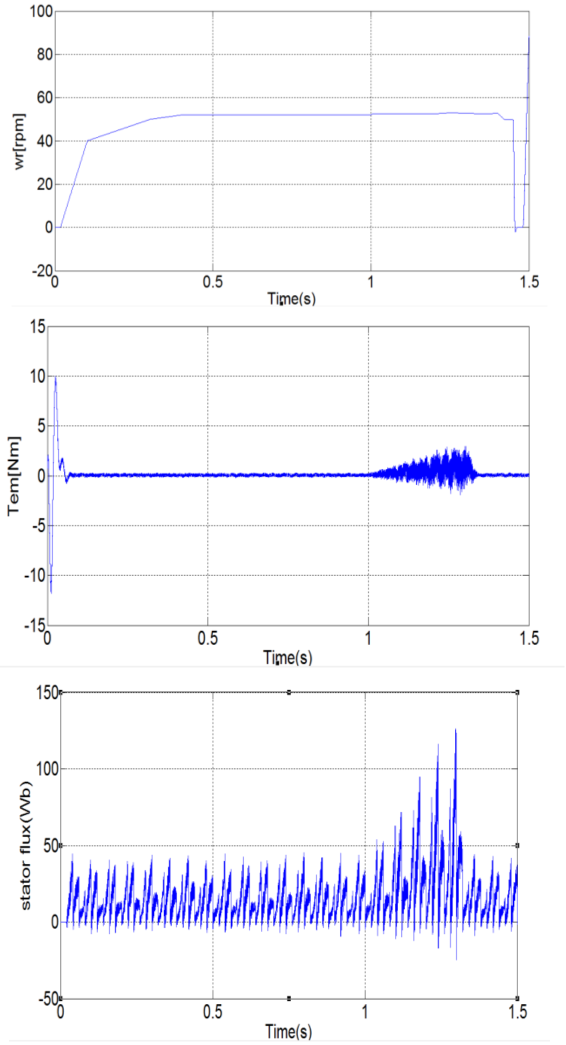

Figure 10. Robustness test of the proposed method under light torque and low speed condition

VI. PROPOSED RESULTS:

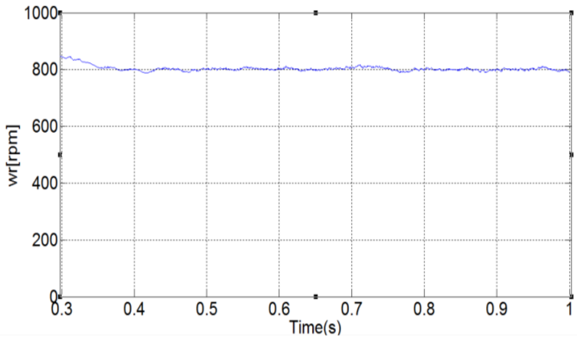

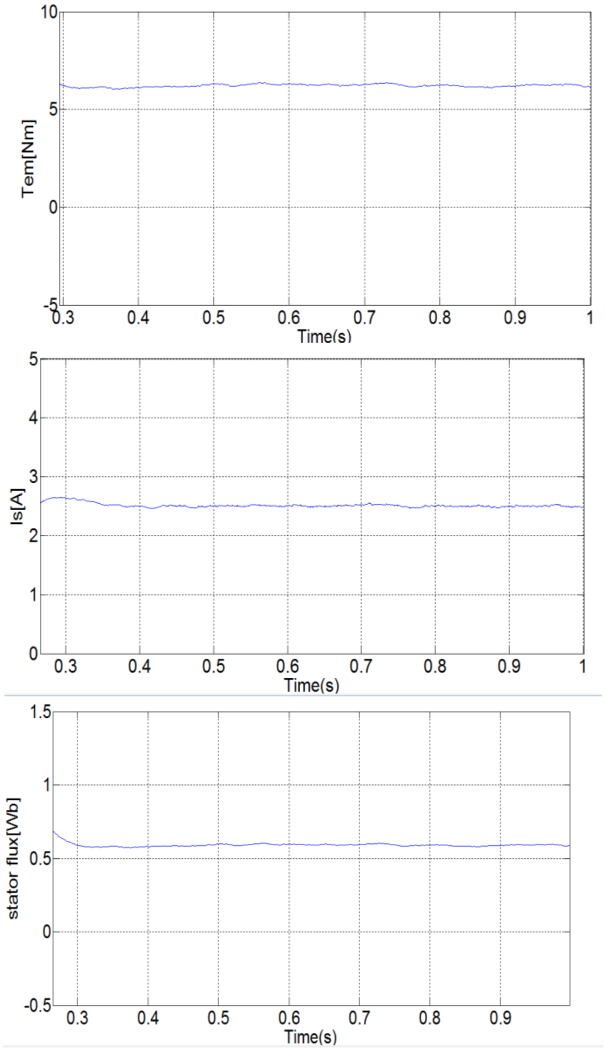

Figure 11. Steady state responses of the proposed method

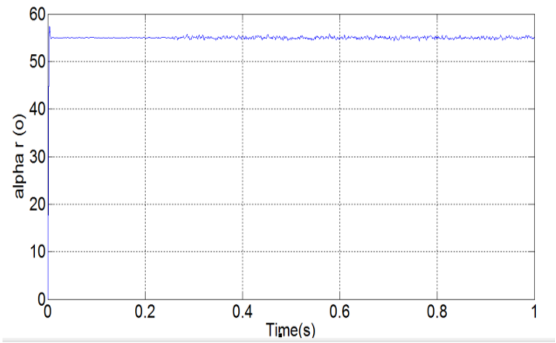

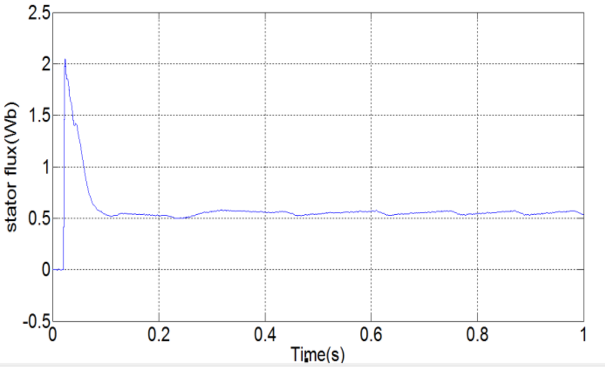

Figure 12. Dynamic state response of the proposed method

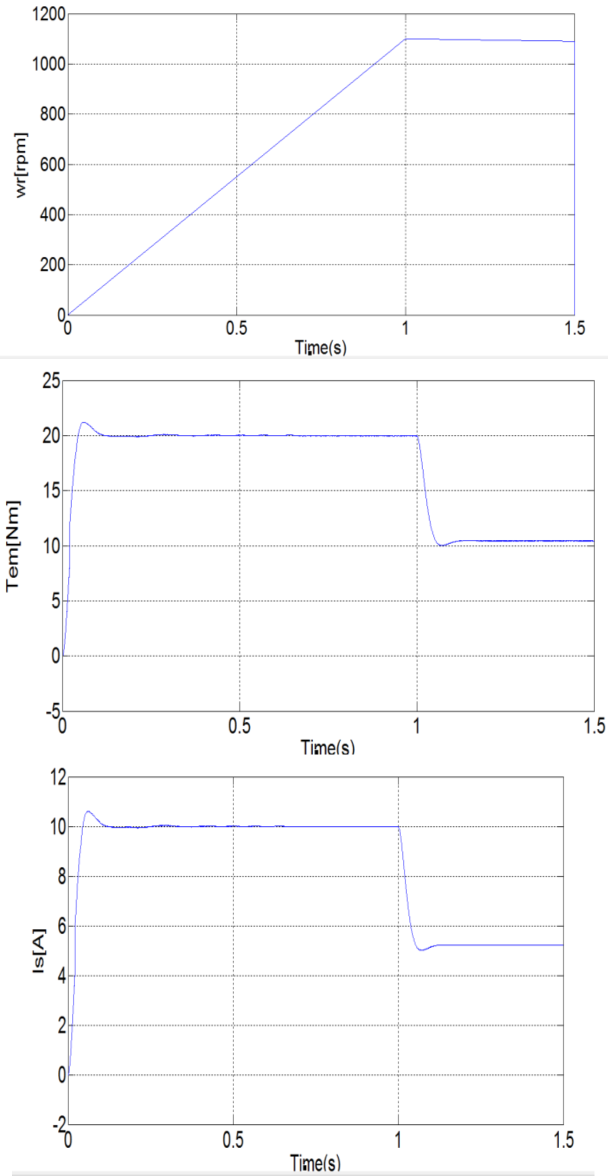

Figure 13. Full load condition responses of proposed method

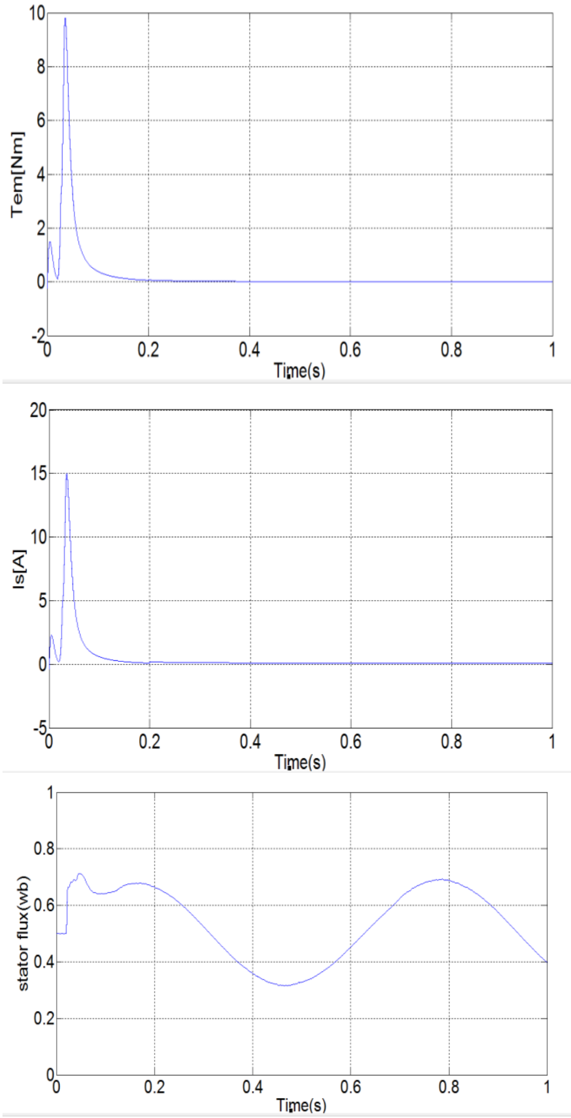

Figure 14. Light load condition responses of the proposed predictive direct angle control

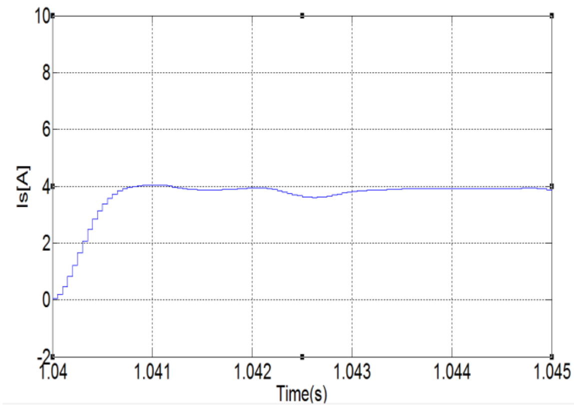

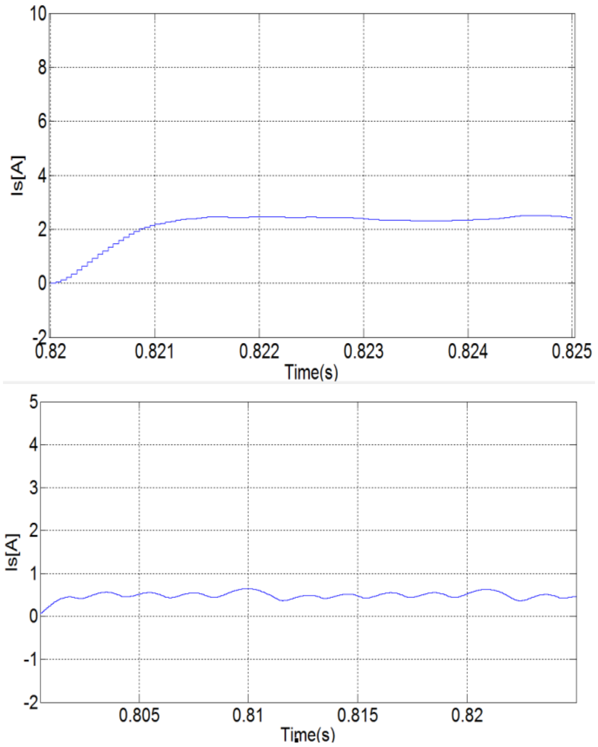

Figure 15. Stator current comparison under (a) full load, (b) mean load, and (c) light load condition

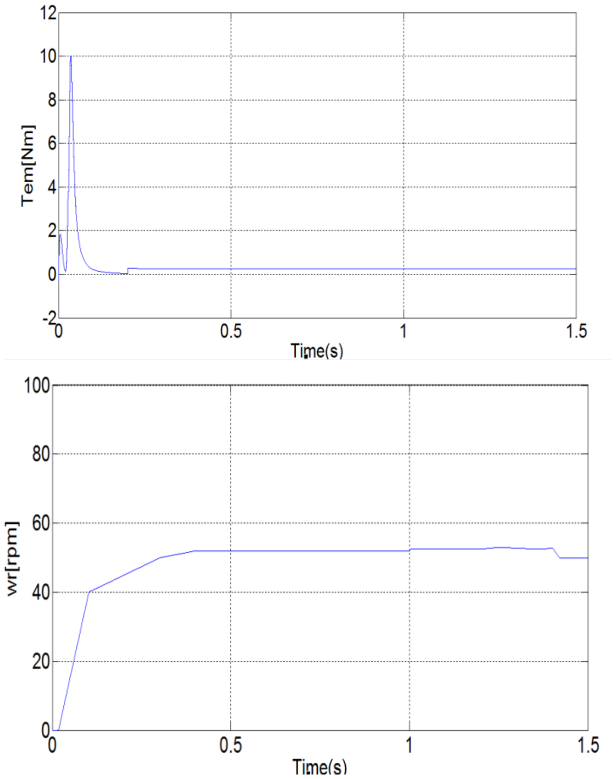

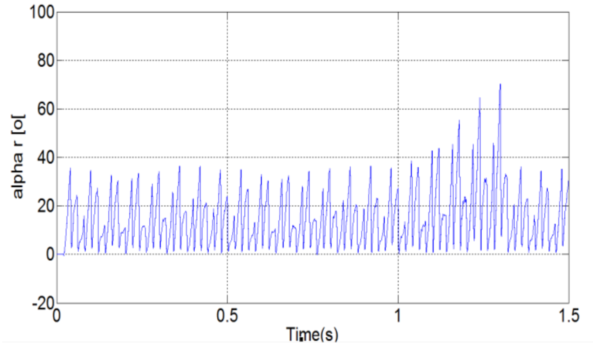

Figure 16. Robustness test of the proposed method under light torque and low speed condition

VII. CONCLUSION

In this paper is to presents a survey of available DAC-MLI techniques for induction motor drives. DAC speaks to a suitable contrasting option to vector control. The primary describe of DAC is straightforward and strong control structure since it doesn't require facilitate changes . A novel limited set predictive direct prediction control strategy is proposed in this paper. The flux is not specifically controlled in this technique. Rather, the torque and the stage prediction contrast between the stator current and the rotor flux are controlled. The stage point is controlled on 45°. This will limit the current and advance the flux consequently. The forecast count is performed in stationary prediction. Likewise, the cost work minimization is performed by considering the discrete idea of the inverter. Therefore, the prediction control ends up noticeably conceivable without utilizing fast processors. By using diode clamped Multilevel inverter the Constant switching frequency schemes considerably improve the drive performance in terms of reduced torque and flux pulsations, reliable start up, well-defined harmonic spectrum and radiated noise. Therefore, an excellent solution for general purpose IM drives in a very wide power range.

A closed loop expectation show is utilized for a precise prediction forecast. Post moving technique is used for input pick up count. A robust strategy is utilized to trade off between the quickness and power of the expectation display. The proposed should is assessed by methods for simulations and examinations. The strategy spans to littler streams contrasted with traditional technique in low speed and light torque area. In any case, it doesn't demonstrate any noteworthy change in nominal point. The strategies robust are kept in low speed area. It is more powerful in low speed and light torque directs looked at toward low speed and high torque focuses.

VIII. REFERENCES

[1]. P. Correa, M. Pacas, and J. Rodriguez, “Predictive torque control for inverter-fed induction machines,” IEEE Trans. Ind. Electron., vol. 54,no. 2, pp. 1073–1079, Apr. 2007.

[2]. S. A. Davari and D. A. Khaburi, “Sensorless predictive torque control by means of sliding mode observer,” IEEE Int. Conf. Power Energy Conf., Dec. 2008, pp. 707–711.

[3]. A. Linder, R. Kanchan, R. Kennel, and P. Stolze, Model-Based PredictiveControl of Electric Drives. G¨ottingen, Germany:CuvillierVerlag, 2010.

[4]. R. Kennel, A. Linder, and M. Linke, “Generalized predictive control (GPC)-ready for use in drive applications,” IEEE 32nd Annu. PowerElectron. Spec. Conf., 2001, pp. 1839–1844.

[5]. R. Vargas, J. Rodrıguez, U. Ammann, and P. W. Wheeler, “Predictive current control of an induction machine fed by a matrix converter withreactive power control,” IEEE Trans. Ind. Elecron., vol. 55, no. 12, pp. 4372– 4380, Dec. 2008.

[6]. R. Vargas, U. Ammann, B. Hudoffsky, J. Rodriguez, and P. Wheeler “Predictive torque control of an induction machine fed by a matrix converter with reactive input power control,” IEEE Trans. Ind. Electron., vol. 25, no. 6, pp. 1426–1438, Jun. 2010.

[7]. S. Alireza Davari, D. Khaburi, F. Wang, and R. Kennel, “Using full order and reduced order observers for robust sensorless predictive torque control of induction motors,” IEEE Trans. Power Electron., vol. 27, no. 7, pp. 3424–3433, Jul. 2012.

[8]. S. A. Davari, D. A. Khaburi, and R. Kennel, “An improved FCS-MPC algorithm for induction motor with imposed optimized weighting factor,” IEEE Trans. Power Electron., vol. 27, no. 3, pp. 1540–1551,Mar. 2012.

[9]. F. Wang, Z. Zhang, S. A. Davari, R. Fotouhi, D. A. Khaburi, J. Rodriguez, and R. Kennel, “An Encoderless Predictive Torque Control for an Induction Machine With a Revised Prediction Model and EFOSMO,” IEEE Trans. Ind. Electron., vol. 61, no. 12, pp. 6635-6644,Dec. 2014.

[10]. S. Bolognani, L. Peretti, and M. Zigliotto, “Torque Feedforward Control Technique for Permanent-Magnet Synchronous Motors,” IEEE Trans. Ind. Electron., vol. 26, no. 11, pp. 20-28, Jan. 2011.

[11]. B. Cheng, and T. R. Tesch, “Online MTPA Control Strategy for DTC Synchronous-Reluctance-Motor Drives,” IEEE Trans. Ind. Electron., vol. 57, no. 3, pp. 969-974, Mar. 2010.

[12]. M. F. Rahman, L. Zhong, and K. W. Lim,, “A Direct Torque-Controlled Interior Permanent Magnet Synchronous Motor Drive IncorporatingField Weakening,” IEEE Trans. Ind. Appl., vol. 34, no. 6, pp. 1246- 1253, Nov/Dec. 1998.

[13]. S. Bolognani, R. Petrella, A. Prearo, and L. Sgarbossa, “Automatic Tracking of MTPA Trajectory in IPM Motor Drives Based on AC Current Injections,” IEEE Trans. Ind. Appl., vol. 47, no. 1, pp. 105-114, Jan/Feb. 2011.

[14]. M. Preindl, and S. Bolognani “Model Predictive Direct Speed Control with Finite Control Set of PMSM Drive Systems,” IEEE Trans. Power Electron., vol. 28, no. 2, pp. 1007-1016, Feb. 2013.

[15]. M. Preindl, and S. Bolognani “Model Predictive Direct Torque Control With Finite Control Set for PMSM Drive Systems, Part 1: Maximum Torque Per Ampere Operation,” IEEE Trans. Ind. Inf., vol. 9, no. 4, pp. 1912-1621, Nov. 2013.

[16]. M. Preindl, and S. Bolognani “Model Predictive Direct Torque Control With Finite Control Set for PMSM Drive Systems, Part 2: FieldWeakening Operation,” IEEE Trans. Ind. Inf., vol. 9, no. 2, pp. 648-657 May. 2013.

[17]. J. F. Stumper, A. Dotlinger, R. Kennel, “Loss Minimization of Induction Machines in Dynamic Operation,” IEEE Trans. Energy Conv., vol. 28, no. 3, pp. 726-735, May. 2013.

[18]. P. Vas, “Sensorless Vector and Direct Torque Control,” OXFORD University Press, 1998.19C. Lascu, and G.Andreescudd, “Sliding-Mode Observer and Improved Integrator With DC-Offset Compensation for Flux Estimation in Sensorless-Controlled Induction Motors,” IEEE Trans. Ind. Electron., vol. 53, no. 3, pp. 785-794, June. 2006.

[19]. J. R. Dominguez, “Discrete-Time Modeling and Control of Induction Motors by Means of Variational Integrators and Sliding Modes—Part I:

Mathematical Modeling," IEEE Trans. Ind. Electron., vol.62, no.9, pp.5393-5401, Sept. 2015.

ABOUT AUTHORS:

Ms. D.sree lakshmi completed B.Tech in EEE from Ravindra Engineering College for women Kurnool in 2014. she is currently doing M.Tech in JNTUA college of Engineering, Anantapuram.her areas of interests are Power Electronics and power systems.

Ms. B.Thejasvi completed B.Tech in EEE from gates engineering college gooty in 2009, and M.Tech from GPRE College, Kurnool in 2011.She is currently working as a Lecturer, EEE Department, JNTUA College of Engineering, Anantapuram. Her areas of interests are power electronics, electrical machines and control systems.